Journal of Physics:
Conference Series

Fluctuation spectroscopy of iron-based superconductors $Ba(Fe_{1-x}Co_x)_2As_2$

To cite this article: Marvin Kopp *et al* 2026 *J. Phys.: Conf. Ser.* **3161** 012018

Journal of Physics: Conference Series **3161** (2026) 012018 doi:10.1088/1742-6596/3161/1/012018

Fluctuation spectroscopy of iron-based superconductors $Ba(Fe_{1-x}Co_x)_2As_2$

Marvin Kopp[1], Charu Garg[1], Markus König[2], Thomas Wolf[3], Amir-Abbas Haghighirad[3], Matthieu Le Tacon[3] and Jens Müller[1]

[1]Institute of Physics, Goethe-Universität Frankfurt, Frankfurt (Main), Germany
[2]Max-Planck-Institut für Chemische Physik fester Stoffe, Dresden, Germany
[3]Institute for Quantum Materials and Technologies, Karlsruher Institut für Technologie, Karlsruhe, Germany

E-mail: kopp@physik.uni-frankfurt.de

Abstract. Nematicity and its influence on the superconducting phase in $Ba(Fe_{1-x}Co_x)_2As_2$ is still a major research interest as the origin of unconventional superconductivity in iron pnictides is still under debate. One of the remaining questions is how the magnetic and structural transitions, with nematic fluctuations extending over a wide temperature range, influence the charge carrier dynamics in particular at low frequencies. We present resistance fluctuation measurements on high-quality $Ba(Fe_{1-x}Co_x)_2As_2$ samples, made possible by cutting a meander structure into the sample by means of a focused ion beam. The preparation process is described and the resulting temperature-dependent noise properties of three different substitution levels ($x = 0\,\%$, $x = 4\,\%$ and $x = 6\,\%$) are presented. We observe only small changes in the noise amplitude in the vicinity of the nematic transition temperatures. However, a larger feature in the ordered phase of the $x = 4\,\%$ doped sample is detected, which may be related to a strong coupling of the charge carriers to lattice modes at domain walls. Future work on straining and detwinning the samples, as well as an anisotropy analysis of the fluctuations on one and the same sample, may allow to clarify the results.

1 Introduction

Superconductivity, in particular at relatively high temperatures, has been a subject of continuing interest in fundamental research over the past decades, as it holds great promise to revolutionize modern technologies if a stable superconductor at room temperature can be found. To achieve this goal, a fundamental understanding of the underlying processes in superconductors is required. In particular unconventional superconductors, which often exhibit higher transition temperatures than conventional superconductors, with complex ground states and multiple phases influencing their superconducting transition, are studied in great detail. One of these material classes are the iron-pnictides superconductors discovered in 2008 [1], which were the first materials besides copper-oxide-based superconductors to show unconventional superconductivity at high temperatures, leading physicists to believe that high-temperature superconductivity is not limited to one class of materials, but to more general conditions [2].

In this study we focus on $Ba(Fe_{1-x}Co_x)_2As_2$, which in its pure form ($x = 0$) exhibits a striped magnetic order below $T_N = 134\,K$ accompanied by a structural transition and shows no superconductivity at low temperatures. Electron or hole doping then leads to more unusual spin configurations and superconductivity. In the case of cobalt substitution, the system is doped with electrons and a splitting of the

magnetic and structural transition temperatures occurs. Upon cooling, the structure first changes from tetragonal to orthorhombic, breaking rotational but not translational symmetry. The latter is then broken at the magnetic transition upon further cooling, leaving an intermediate phase [3]. Borrowed from liquid crystal physics, this state has been termed the electronic nematic phase and can be distinguished in, e.g., resistance (see below) or specific heat measurements [4], and especially in elastic shear modulus measurements [5]. Further experiments have found evidence for nematic fluctuations extending far across the phase diagram [6], provoking the question of the role of nematic fluctuations in the formation of superconductivity, which occurs with sufficient hole doping. The phase diagram of $Ba(Fe_{1-x}Co_x)_2As_2$ is shown in Fig.1(a).
The nematic state has been extensively studied by transport, optical, shear modulus and many other measurements [7, 8, 9, 10]. Here we report on first resistance fluctuation measurements on bulk samples. Fluctuation (or noise) spectroscopy quantifies the charge carrier fluctuations and provides insight into their changing dynamics and sometimes the underlying microscopic processes [11, 12]. Essentially, a time-resolved resistance measurement is performed, the signal of which is transformed into frequency space using a Fourier transformation, yielding the power spectral density (PSD) of the resistance fluctuations. This PSD is directly related to the autocorrelation function of the system and, via fluctuation-dissipation relations, to the imaginary part of the corresponding dynamic susceptibility [11]. The frequency dependence of the PSD spectra of $1/f$-type can be evaluated and interpreted in frequency ranges from mHz to kHz, depending on the observed type of noise and measurement time. In solid state physics $1/f$ or so-called "flicker noise" is predominantly observed and has been of great interest to researchers in the past decades [13, 14, 15]. There, the PSD increases towards lower frequencies with a given exponent $S_R \propto 1/f^{\alpha}$ where α takes values between 0.8 and 1.4, yielding valuable information about the spectral weight distribution of the charge carrier dynamics coupled to different electric, magnetic or structural degrees of freedom [16].

2 Experimental Details

High-quality single crystals of $Ba(Fe_{1-x}Co_x)_2As_2$ were grown from self-flux in a glassy carbon or an alumina crucible. Low cooling rates of $\sim 1\,°C/h$ were used to minimize the amount of flux inclusions and crystal defects. The composition of the crystals were determined by a benchtop scanning electron microscope (SEM) and energy dispersive x-ray spectroscopy (EDX) (COXEM EM-30AXN). Electrical transport measurements on single crystals have been carried out using an AC technique and a lock-in amplifier. The AC voltage is applied to a voltage divider circuit with a limiting resistor much larger than the sample resistance. Resistance measurements were conducted in a four-terminal setup and the resistance noise spectroscopy in a five-terminal setup.
The samples were exfoliated to obtain an oxygen-free surface, resulting in good electrical contacts using gold wires and a silver conductive paste. Preliminary measurements indicated that the highly metallic behavior of the $Ba(Fe_{1-x}Co_x)_2As_2$ crystals makes noise spectroscopy measurements increasingly difficult, if not impossible, in certain temperature ranges, since the noise magnitude is found to be proportional

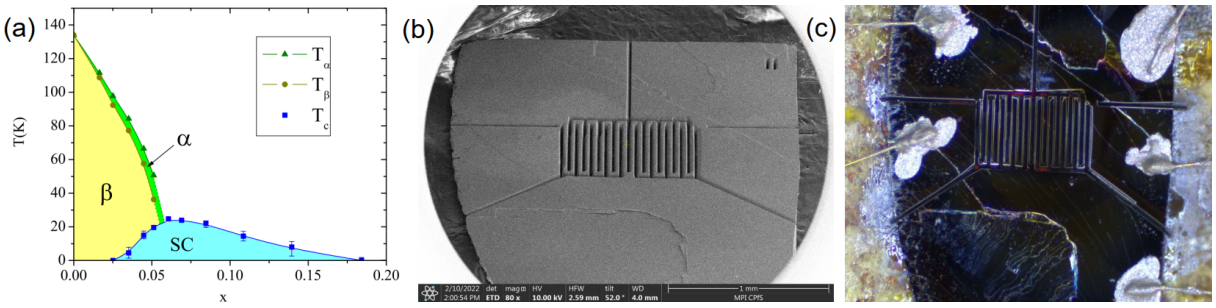

Figure 1: Phase diagram of electron doped $Ba(Fe_{1-x}Co_x)_2As_2$ in (a), reprinted from [4] with permission of the American Physical Society. Pictures of a micro-structured $Ba(Fe_{1-x}Co_x)_2As_2$ sample under an electron microscope in the FIB (b) and under an optical microscope after contacting with gold wires and conducting silver paste (c). Note the fifth middle contact leading to a highly symmetrical setup used in the measurements.

to the absolute resistance of the measured sample squared [17]:

$$S_R = \frac{\gamma_H \cdot R^2}{n_c \Omega f^\alpha} \,. \tag{1}$$

This so-called Hooge's Law has been empirically proven and predicts a PSD that is dependent on a material specific parameter γ_H, the absolute resistance R squared, the inverse of the charge carrier concentration n_c, the noisy volume of the sample Ω and the frequency f with an exponent α being close to 1. Substituting the absolute resistance with the resistivity and assuming a cuboid sample, it becomes obvious that a longer and especially thinner current path would greatly improve the noise magnitude and make measurements feasible even for low-impedance metallic samples ($S_R \propto l/A^3$, where l is the lenght of the pass and A the cross sectional area) [18].
A possible way to achieve those traits without altering the sample properties is to fabricate a micro-structured meander pattern into a single crystal using a focused ion beam (FIB). Just before the cutting process in a xenon plasma FIB, the samples were exfoliated and afterwards contacted with gold wires and a conductive silver paste. In Fig. 1(b) one of the samples is shown just after the cutting process using an electron microscope in the FIB chamber and in (b) after making electrical contacts. The samples were glued on a copper block using GE varnish and electrically isolated. This technique has been demonstrated for a low-impedance heavy fermion system in [18]. The pictures also show that we added a fifth contact in the middle of the meander structure for perfect symmetry. This allows the sample itself to be used as a kind of Wheatstone bridge to suppress the voltage offset caused by the resistance and to eliminate fluctuations from the current source and temperature bath [19]. The balanced voltage is then amplified by a low-noise preamplifier before it is processed by the lock-in and the voltage noise PSD of the emerging fluctuations is calculated by a spectrum analyzer [12, 20, 21]. All fluctuation spectroscopy results shown in the following were obtained by measuring in a five-point configuration in a cross-correlation setup, where the signal is split and processed by two preamplifiers and two lock-ins simultaneously. The cross-correlation spectrum of both signals is then calculated by the signal analyzer, eliminating the uncorrelated fluctuation contributions from amplifier and lock-in.

3 Results and Discussion

Initial resistance measurements of an undoped ($x = 0$) $Ba(Fe_{1-x}Co_x)_2As_2$ single crystal without patterning are presented in Figure 2 (a) in blue. Starting at high temperatures the absolute resistance

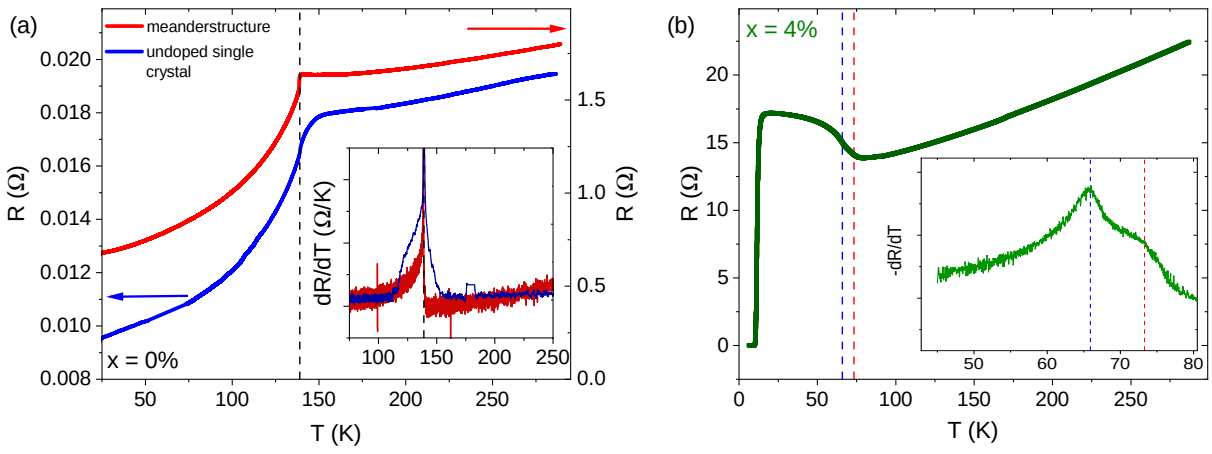

Figure 2: (a) Resistance of a unaltered single crystal of undoped $Ba(Fe_{1-x}Co_x)_2As_2$ in blue compared to a meander structured sample in red with resistance values almost 100 times larger. The inset shows the derivative of both measurements. In (b) the resistance and derivative of the resistance (inset) of a doped sample is shown to clarify the evaluation of transition temperatures.

amounts to $R(300\,\mathrm{K}) \approx 20\,\mathrm{m\Omega}$ and shows the characteristic metallic decrease upon cooling with a change in slope near the structural and magnetic transition temperature $T_{\mathrm{N,S}} = 139\,\mathrm{K}$. The unprocessed single crystal shows a relatively broad transition with onset at about $T \approx 155\,\mathrm{K}$ as seen in the inset. In direct comparison, the resistance of a meander-structured single crystal fabricated as described in section 2 is

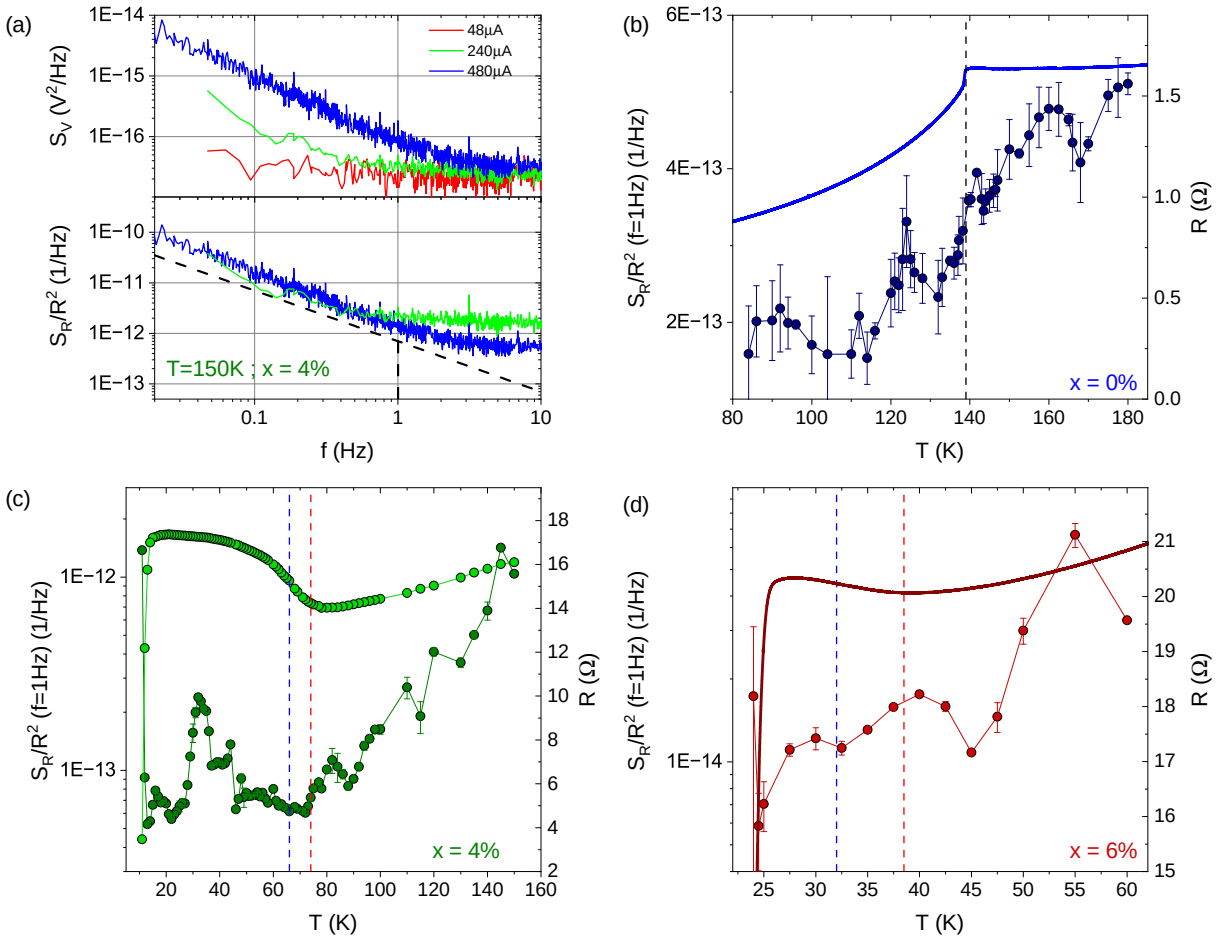

Figure 3: Exemplary noise spectra at $T = 150\,\mathrm{K}$ for different currents shown in (a) for the raw voltage fluctuations $S_V(f)$, upper panel, and the normalized quantity $S_R/R^2(f)$, lower panel, with dotted lines representing a perfect $1/f$ behavior and $f = 1\,\mathrm{Hz}$. (b),(c) and (d) picture the temperature-dependent resistance and normalized noise amplitude $S_R/R^2(T, f = 1\,\mathrm{Hz})$ for $x = 0\,\%$, $x = 4\,\%$ and $x = 6\,\%$ respectively.

shown in red. The same qualitative temperature dependence is observed, but the absolute resistance is almost two orders of magnitude larger compared to the unpatterned single crystal, thereby improving the resolution of the experiment, especially the noise measurements. The drop in resistance is now clearly visible at $T_{\mathrm{N,S}} = 139\,\mathrm{K}$ marked by the dotted line in the resistance, as well as the derivative. In Fig. 2(b) the resistance of a doped sample $x = 4\,\%$ is shown to highlight the difference in resistance behavior with doping and the splitting of the two transition temperatures. Here the absolute resistance is even higher (almost one order of magnitude) which can be attributed to an improved manufacturing process of the meander structure and a larger sample, allowing for a longer structure. Here, the resistance also shows a metallic behavior at high temperatures but then starts to increase below $T \approx 80\,\mathrm{K}$ with two distinct slope changes before the expected superconducting transition at $T_c = 15\,\mathrm{K}$. The two distinct slope changes, marked in the temperature derivative of the resistance shown in the inset, are interpreted as the structural transition (nematic, red dotted line) at $\mathrm{T_S} = 74\,\mathrm{K}$ and the magnetic transition (blue dotted line) $T_{\mathrm{N}} = 66\,\mathrm{K}$ after [22]. It is important to note, that the samples are not detwinned and further studies of the electronic anisotropy are planned on detwinned samples in the future.
In Fig. 3(a) exemplary fluctuation spectra measured on the $x = 4\,\%$ doped sample at $T = 150\,\mathrm{K}$ demonstrate the feasibility of the measurements. According to Eq.(1) the power spectral density of the voltage fluctuations should be current-dependent as shown in the upper graph. For a small current of $I = 48\,\mu\mathrm{A}$ (red) no frequency dependence is observed and therefore only the white background of the measurement

setup is observed. Only at higher currents a $1/f$-dependence at lower frequencies becomes visible and the signal of the sample is observed. In the lower graph the normalized quantity of the same spectra $S_R/R^2(f)$ is plotted and, as expected, the $1/f$ part is current independent, proving that the signal is intrinsic. The dotted line is a guide to the eye and depicts a perfect $1/f$ behavior. The value at $f = 1\,\mathrm{Hz}$ is marked to clarify our analysis procedure. The increase in absolute resistance makes measurements of the noise PSD possible and allows the analysis of $1/f^{\alpha}$-type spectra extracting the slope α and the noise amplitude at $f = 1\,\mathrm{Hz}$ in order to quantify the temperature dependence of the measured fluctuations. Changes of the frequency exponent reflects a shift in spectral weight of the fluctuators. A homogeneous distribution of the fluctuator energies corresponds to $\alpha = 1$ and deviations indicate a shift to slower ($\alpha > 1$) or faster fluctuations ($\alpha < 1$) [20].

The results for three selected samples with different doping levels are shown in Fig. 3, where the resistance and normalized noise PSD $S_R/R^2(f = 1\,\mathrm{Hz})$ are shown for $x = 0\,\%$ in (b) (blue), for $x = 4\,\%$ in (c) (green) and for $x = 6\,\%$ in (d) (red). As mentioned above, the absolute resistance and thus the resolution of the measurements was lowest for the $x = 0\,\%$ sample, as the meander structure was the shortest. For all three samples, the normalized resistance noise amplitude is overall very small (for reference the noise floor in a standard four-terminal lock-in AC measurement setup is about $S_R/R^2(f = 1\,\mathrm{Hz}) \approx 10^{-11}\,\mathrm{Hz}^{-}1$) and are only measurable due to the described improvements in sample geometry and measurement setup in section 2. Upon cooling down, the noise level decreases for all three samples up to a certain temperature preceding the first phase transition. For the undoped sample, a small maximum at $T = 160\,\mathrm{K}$ is observed, before the noise amplitude continues to decrease through the transition down to $T = 132\,\mathrm{K}$. Here the noise level begins to increase again up to a second local maximum at $T = 124\,\mathrm{K}$ in the ordered phase, after which the noise level drops and remains roughly constant at lower temperatures. Besides the small peak just above T_N there is no major signature in the low-frequency fluctuations at the phase transition.

The most detailed measurements with very small temperature increments were performed on the $x = 4\,\%$ doped sample, where the nematic phase is nicely observed in the resistance and which becomes superconducting at low temperatures. The overall trend of the temperature-dependent noise amplitude is similar to the undoped sample with a decrease upon cooling in the metallic phase, a small peak at $T = 82\,\mathrm{K}$ preceding the nematic transition at $T_S = 74\,\mathrm{K}$ (red dotted line). No large changes are observed in the nematic phase and the noise amplitude remains constant down to a pronounced peak in the ordered phase at $T = 32\,\mathrm{K}$, which we will discuss in more detail below. At the superconducting transition the normalized noise amplitude starts to rise significantly. For the $x = 6\,\%$ doped sample in (d) there may be a small increase at higher temperatures before the same decreasing trend in the metallic phase sets in down to $T = 45\,\mathrm{K}$. The small maximum at $T = 40\,\mathrm{K}$ is broader here with the decrease in noise amplitude now extending through the nematic phase from $T_S = 38.5\,\mathrm{K}$ down to the magnetic transition $T_\mathrm{N} = 32\,\mathrm{K}$ (blue dotted line). In the ordered phase, the PSD amplitude remains constant for a few Kelvin before further decreasing below $T = 28\,\mathrm{K}$ followed by an increase at the superconducting transition.

Besides the noise magnitude, the second parameter to analyze in $1/f^{\alpha}$-type noise is the frequency exponent α. We show this analysis in detail for the $x = 4\,\%$ doped sample in Fig. 4, where in (a) the same PSD is again plotted and in (b) the corresponding frequency exponent. The noise level and the frequency exponent initially decrease from values larger than one upon cooling until α starts to increase and becomes greater than one again around $T = 100\,\mathrm{K}$, indicating a slowing down of the dynamics (shift to lower frequencies) and the PSD saturates around $S_R/R^2 \approx 10^{-13}\,\mathrm{Hz}^{-1}$. Just before the nematic transition we observe another small feature in both the PSD and frequency exponent. The effect is more pronounced at lower temperatures, where a pronounced change in the charge carrier fluctuations is observed starting at $T = 44\,\mathrm{K}$. Here the noise amplitude shows a broad maximum and α first drops below 1 and then exhibits a larger peak before dropping again indicating a shift in spectral weight to lower frequencies within a small temperature range.

A possible explanation for describing the ubiquitous $1/f$ noise in solids is a superposition of independent two-level processes fluctuating with a characteristic time constant τ and coupled to the resistance of the system. In case of thermally activated processes, the relaxation time follows an Arrhenius law $\tau_c = \tau_0 \exp\left(E_A/(k_B T)\right)$, where τ_0 denotes an attempt time, typically of order the inverse phonon frequencies (10^{-14}-$10^{-11}\,\mathrm{s}$), and E_A denotes the a characteristic energy of the two-level potential. The superposition of Lorentzian spectra with a sufficiently broad distribution of activation energies $D(E_A) \equiv D(E)$ then leads to a $1/f^{\alpha}$-type spectrum [23] in a frequency window determined by the energy distribution. A phenomenological model based on this concept of non-exponential kinetics [1] was introduced by Dutta,

[1] The correlation function of a two-level process decays exponentially with a characteristic time τ_c. The superposition of many such processes, however, results in a non-exponential dynamics.

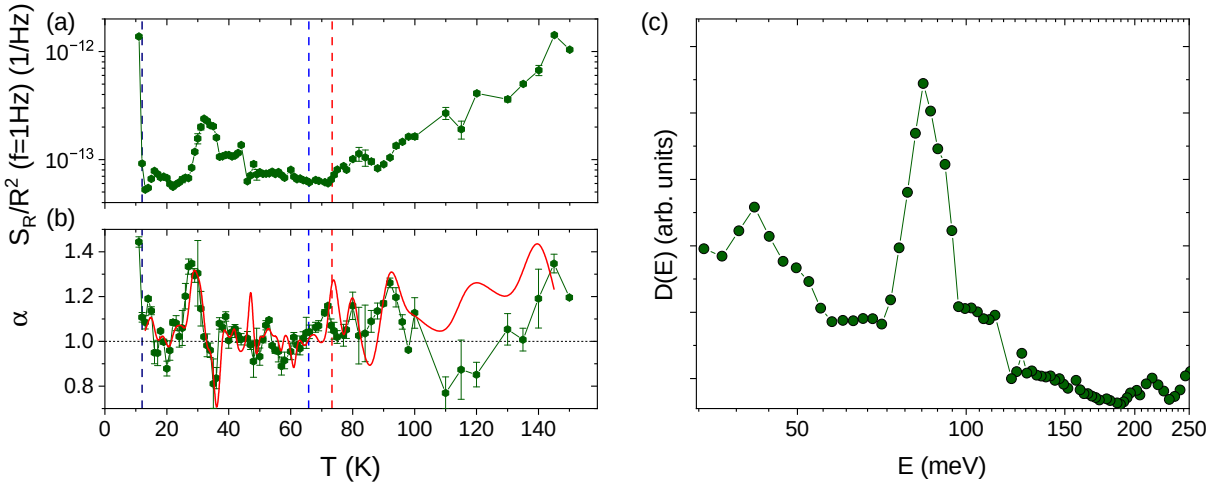

Figure 4: Noise amplitude and frequency exponent α of the $x = 4\,\%$ sample in (a) and (b). With the frequency exponent the theoretical prediction of the DDH model is shown in red. The calculated energy distribution from this model is shown in (c) where the peak at $T = 32\,\mathrm{K}$ corresponds to $E = 84\,\mathrm{meV}$.

Dimon and Horn (DDH) [24]. Under the assumption that the same fluctuation processes determine the temperature dependencies of both the noise magnitude, shown in Fig. 4 (a), and the frequency exponent (spectral weight distribution), the model predicts [25, 26]

$$\alpha(T) = 1 - \frac{1}{\ln(2\pi f \tau_0)} \left[\frac{\partial \ln(S(f,T))}{\partial \ln(T)} - \frac{\partial \ln(g(T))}{\partial \ln(T)} - 1 \right], \tag{2}$$

where $g(T)$ accounts for an explicit temperature dependence of the distribution of activation energies. The calculated frequency exponent α according to the DDH model is shown in red in Fig 4(b) and shows that it describes the experimental data rather well below $T \approx 100\,\mathrm{K}$. Here a time constant $\tau_0 = 1 \cdot 10^{-14}\,\mathrm{s}$ and $g(T) = T^2$ where used, indicating a weak temperature dependence of the coupling between fluctuators and resistance. Since experimental data and model fit very well for temperatures below $T \approx 50\,\mathrm{K}$, the energy distribution $D(E)$ can be calculated after:

$$D(E) \propto \frac{2\pi f}{k_B T} \frac{S_R(f,T)}{R^2}, \tag{3}$$

and is shown in Fig. 4(c). There $E = -k_\mathrm{B} T \ln(2\pi f \tau_0)$ corresponds to the energy of the fluctuators composing the $1/f$ noise and the two maxima correspond to energies $E = 84\,\mathrm{meV}$ and $E = 42\,\mathrm{meV}$. In the model, no explicit microscopic origin of the $1/f$ noise is assumed and corresponding energy scales have to be confirmed a posteriori to deduce the underlying processes. In the closely related compound FeSe for example, J. Jandke *et al.* discuss the coupling of low-energy electrons to phonons and find an enhanced coupling close to domain boundaries in this energy range [27]. They emphasize that this is a local effect and that results of spatially averaging effects (such as mean resistance measurements) should be taken with caution. Resistance noise, however, is rather sensitive to local excitations. Still, we are working with samples that are not intentionally detwinned and we do not know the domain structure in the sample.

4 Conclusion and outlook

In summary, we present resistance noise measurements on high-quality $Ba(Fe_{1-x}Co_x)_2As_2$ samples with three different cobalt doping levels. The measurements were possible due to the described structuring process using a focused ion beam to cut a meander structure into a cleaved sample. Depending on the sample size, the absolute resistance of the measured sample is increased by up to two orders of magnitude, thereby enabling fluctuation spectroscopy measurements in the low-frequency range. All three measured samples $x = 0\,\%$, $x = 4\,\%$ and $x = 6\,\%$ show a decrease in the normalized resistance power spectral density $S_R/R^2(T, f = 1\,\mathrm{Hz})$ upon cooling down as well as a small maximum before entering the nematic

phase. At low temperatures the noise amplitude stays roughly constant, before we observe a strong increase in the vicinity of the superconducting transition temperature, which has been observed in other systems before [28, 29]. The results of detailed noise measurements on the $x = 4\,\%$ doped sample are presented, where both nematicity and superconductivity are observed in the resistance measurements. We find a pronounced peak in the noise in the ordered phase, which is well described by the DDH model. The agreement between model and experimental data in the temperature regime of the maximum at $T = 32\,\mathrm{K}$ allows to determine the energy scale of the underlying fluctuation processes to $E \approx 84\,\mathrm{meV}$. Similar energy scales have been observed in optical measurements by J. Jandke *et al.* in single layer FeSe and have been interpreted as a strong coupling of charge carriers and lattice modes at domain borders [27]. Since our samples are not detwinned, a future goal is to establish fluctuation spectroscopy measurements on meander-structured and strained samples to be able to distinguish between structural domain fluctuations and nematic effects. After G. Drachuck *et al.*, it should be possible to observe long-lived "topotwin-domains" that form in the sample depending on the applied strain. Those domains should lead to slow fluctuations which fluctuation spectroscopy will be able to reveal (the experimental part of the paper has been retracted but the theory is still valid [30]). To quantify this effect, we suggest to develop a microstructure pattern that allows for anisotropy measurements of both resistance and noise properties.

5 Acknowledgments

We acknowledge support from the Deutsche Forschungsgemeinschaft (DFG, German Research Foundation) through the Transregional Collaborative Research Center TRR 288 - 422213477 (projects B02, B03 and A10).

References

[1] Y. Kamihara et al. "Iron-Based Layered Superconductor La[$O_{1-x}F]_x$FeAs (x = 0.05-0.12) with Tc = 26 K". In: *Journal of the American Chemical Society* 130.11 (2008). PMID: 18293989, pp. 3296–3297.

[2] I. I. Mazin. "Superconductivity gets an iron boost". In: *Nature* 464.7286 (Mar. 2010), pp. 183–186.

[3] R. M. Fernandes and J. Schmalian. "Manifestations of nematic degrees of freedom in the magnetic, elastic, and superconducting properties of the iron pnictides". In: *Superconductor Science and Technology* 25.8 (July 2012), p. 084005.

[4] J.-H. Chu et al. "Determination of the phase diagram of the electron-doped superconductor $Ba(Fe_{1-x}Co_x)_2As_2$". In: *Phys. Rev. B* 79 (1 Jan. 2009), p. 014506.

[5] A. E. Böhmer and C. Meingast. "Electronic nematic susceptibility of iron-based superconductors". In: *Comptes Rendus. Physique* 17.1-2 (2016), pp. 90–112.

[6] R. M. Fernandes et al. "Iron pnictides and chalcogenides: a new paradigm for superconductivity". In: *Nature* 601.7891 (Jan. 2022), pp. 35–44.

[7] M. A. Tanatar et al. "Uniaxial-strain mechanical detwinning of $CaFe_2As_2$ and $BaFe_2As_2$ crystals: Optical and transport study". In: *Phys. Rev. B* 81 (18 May 2010), p. 184508.

[8] J.-H. Chu et al. "In-Plane Resistivity Anisotropy in an Underdoped Iron Arsenide Superconductor". In: *Science* 329.5993 (2010), pp. 824–826.

[9] C.-L. Song et al. "Direct Observation of Nodes and Twofold Symmetry in FeSe Superconductor". In: *Science* 332.6036 (2011), pp. 1410–1413.

[10] S. Kasahara et al. "Electronic nematicity above the structural and superconducting transition in $BaFe_2(As_{1-x}P_x)_2$". In: *Nature* 486.7403 (2012), pp. 382–385.

[11] Sh. Kogan. *Electronic noise and fluctuations in solids.* Cambridge University Press, 1996.

[12] J. Müller. "Fluctuation Spectroscopy: A New Approach for Studying Low-Dimensional Molecular Metals". In: *ChemPhysChem* 12.7 (Mar. 2011), pp. 1222–1245.

[13] R. F. Voss and J. Clarke. "Flicker ($1/f$) noise: Equilibrium temperature and resistance fluctuations". In: *Physical Review B* 13.2 (1976), pp. 556–573.

[14] M. B. Weissman. "$1/f$ noise and other slow, nonexponential kinetics in condensed matter". In: *Reviews of Modern Physics* 60.2 (Apr. 1988), pp. 537–571.

[15] T. Thomas et al. "Comparison of the charge-crystal and charge-glass state in geometrically frustrated organic conductors studied by fluctuation spectroscopy". In: *Phys. Rev. B* 105 (20 May 2022), p. 205111.

[16] B. Raquet. "Electronic Noise in Magnetic Materials and Devices". In: *Lecture Notes in Physics*. Springer Berlin Heidelberg, 2001, pp. 232–273.

[17] F. N. Hooge. "1/f noise is no surface effect". In: *Physics Letters A* 29.3 (1969), pp. 139–140.

[18] A. Steppke et al. "Microstructuring $YbRh_2Si_2$ for resistance and noise measurements down to ultra-low temperatures". In: *New Journal of Physics* 24.12 (Dec. 2022), p. 123033.

[19] J. H. Scofield. "ac method for measuring low-frequency resistance fluctuation spectra". In: *Review of Scientific Instruments* 58.6 (1987), pp. 985–993.

[20] J. Müller and T. Thomas. "Low-Frequency Dynamics of Strongly Correlated Electrons in (BEDT-TTF)2X Studied by Fluctuation Spectroscopy". In: *Crystals* 8.4 (2018).

[21] T. Thyzel et al. "Methods in fluctuation (noise) spectroscopy and continuous analysis for high-throughput measurements". In: *Measurement Science and Technology* 36.1 (2024), p. 015501.

[22] I. R. Fisher, L. Degiorgi, and Z. X. Shen. "In-plane electronic anisotropy of underdoped '122' Fe-arsenide superconductors revealed by measurements of detwinned single crystals". In: *Reports on Progress in Physics* 74.12 (Sept. 2011), p. 124506.

[23] F. K. Du Pré. "A Suggestion Regarding the Spectral Density of Flicker Noise". In: *Physical Review* 78.5 (1950), pp. 615–615.

[24] P. Dutta, P. Dimon, and P. M. Horn. "Energy Scales for Noise Processes in Metals". In: *Physical Review Letters* 43.9 (1979), pp. 646–649.

[25] M. B. Weissman et al. "Thermally activated features in $1/f$ noise in silicon on sapphire". In: *Physical Review B* 27.2 (1983), pp. 1428–1431.

[26] D. M. Fleetwood, T. Postel, and N. Giordano. "Temperature dependence of the $1/f$ noise of carbon resistors". In: *Journal of Applied Physics* 56.11 (1984), pp. 3256–3260.

[27] J. Jandke et al. "Unconventional pairing in single FeSe layers". In: *Phys. Rev. B* 100 (2 July 2019), p. 020503.

[28] J. Müller, J. Brandenburg, and J. A. Schlueter. "Magnetic-Field Induced Crossover of Superconducting Percolation Regimes in the Layered Organic Mott System $\kappa-(BEDT-TTF)_2Cu[\mathbf{N}(CN)_2]Cl$". In: *Phys. Rev. Lett.* 102 (4 Jan. 2009), p. 047004.

[29] H. Zi et al. "Resistance fluctuations in superconducting $K_xFe_{2-y}Se_2$ single crystals studied by low-frequency noise spectroscopy". In: *Chinese Physics B* 30.4, 047402 (2021), p. 047402.

[30] G. Drachuck et al. "Dynamic Elastoresistivity Evidence for Slow Nematic Fluctuations in $BaFe_2As_2$". In: *arXiv:1708.02156v1* (2017).